ELSEVIER

Journal of Nuclear Materials 273 (1999) 79–94

journal of nuclear materials

www.elsevier.nl/locate/jnucmat

Modeling and analysis of time-dependent tritium transport in lithium oxide

A. Badawi, A.R. Raffray *, M.A. Abdou

Fusion Technology Group, 43-133 Engineering IV, Department of Mechanical and Aerospace Engineering, University of California, Los Angeles, P.O. Box 951597, Los Angeles, CA 90095-1597, USA

Received 14 July 1993; accepted 17 December 1998

Abstract

Tritium behavior in the solid breeder blanket is one of the key factors in determining tritium self-sufficiency, as well as safety, of fusion reactors. Therefore, it is important to understand the tritium transport mechanisms and processes, in order to accurately determine the tritium release and inventory in the blanket. A model has been developed at UCLA to describe the tritium behavior in solid breeder materials, together with a computer code which can predict the tritium release and inventory. However, the model was limited in some cases: for example, it did not include the capability to account for surface to bulk fluxes and for trapping inside the grain which can have major effects on the tritium transport. The model capabilities have been extended to enable its application over a wide range of experimental conditions. Improvements include: (1) implementing an initial model to account for the general effect of trapping in the bulk, (2) addition of a dissolution flux which would enable a more accurate modeling of solubility driven by hydrogen partial pressure in the solid breeder porosity, (3) inclusion of more hydrogen isotopes species in the pore, and, (4) modification of the existing computer code to allow for broader application, such as the possibility of accounting for both first order and second order adsorption/desorption. The code was used to analyze experimental data on tritium behavior in Li_2O from the BEATRIX-II experiment.

1. Introduction

Attaining self-sufficiency is a critical goal for fusion in order to qualify as one of a very limited number of options for a renewable energy source. If a D–T reactor cannot be tritium self-sufficient, its usefulness in the energy cycle will be very limited since tritium is basically not available from natural sources. Therefore, careful evaluation of the conditions for attaining self-sufficiency is necessary to define the selection criteria for design concepts and the range of acceptable parameters [1]. Tritium behavior and transport in the blanket are particularly important in determining whether self-sufficiency will be achieved. The tritium behavior also determines the width of the operating temperature window for the solid breeder based on acceptable tritium inventory levels. A large inventory is undesirable from both a self-sufficiency as well as a safety point of view. Tritium transport is greatly affected by a number of factors such as [2]:

1. material properties and microstructure,
2. purge gas chemistry, pressure and flow rate,
3. temperature,
4. radiation effects, and
5. lithium burnup.

A model was developed at UCLA by Federici and Raffray [2] to describe the tritium transport behavior in lithium-based ceramic materials. A computer code, named MISTRAL (Model for Investigative Studies of Tritium Release in Lithium Ceramics), was also developed, based on the model. The code had the capability of calculating the tritium release and inventory in transient as well as steady state conditions. MISTRAL was

* Corresponding author. Present address: Fusion Energy Research Program, University of California, San Diego, 460 Engineering Building Unit II, 9500 Gilman Drive, Mail Code 0417, La Jolla, CA 92 093-0417, USA. Tel.: +1-619 534 7716; fax: +1-619 534 9720; e-mail: raffray@fusion.ucsd.edu

0022-3115/99/$ – see front matter
PII: S0022-3115(99)00016-1

based on a model that includes several transport mechanisms, such as diffusion through the grain and grain boundary, surface adsorption and desorption and diffusion along the interconnected porosity. However, other factors that can significantly affect the tritium release and inventory, depending on the material and operating conditions, were not included in the model.

There are three potentially important effects that were neglected and that would need to be added to the original model: (1) dissolution flux from the surface to the bulk, (2) general bulk trapping, for example due to chemical or radiation effect, and (3) the presence of both oxidized and reduced species in the pore.

The need to add the dissolution flux can be clearly seen for example from experiments where no tritium is generated and a Li_2O sample is placed in an atmosphere containing H_2O or H_2. If there is no flux of hydrogen species going into the Li_2O there will be no hydrogen bulk inventory in the sample. The addition of the dissolution flux will tend to increase the surface-driven bulk inventory, which plays an important role in materials with fast diffusion coefficients, such as Li_2O and even $LiAlO_2$, since studies by Raffray et al. [3] suggest that it might also have a fast diffusion coefficient.

It is believed that chemical and/or radiation trapping could have a significant effect on the tritium inventory depending on the operating conditions. For example, Li_2O is known to react with moisture to form LiOH, according to the reversible reaction described by Tetenbaum et al. [4]

$$Li_2O + H_2O = 2LiOH. \quad (1)$$

In the presence of hydroxide radicals in the Li_2O, the diffusive tritium atom could then be trapped in the general form of LiOH, the solubility of which being a function of both the partial pressure of water vapor and the temperature. Under sufficiently high moisture pressure, the LiOH formed would precipitate as a separate phase.

Some of the more recent data available on the tritium release from Li_2O come from the BEATRIX-II experiment (see Ref. [5]), in which Li_2O samples, in the form of rings and cylinders were irradiated and the in situ tritium release was measured under different conditions. Although the tritium inventory was not measured during the experiment, the tritium release was measured. By integrating the release over time, the difference in inventories between two steady states can be calculated. Also the end-of-life tritium inventory was measured. A comparison was made between the modeling results from the original MISTRAL code to the experimental data to determine whether reasonable predictions could be made assuming no bulk trapping. The modeling results substantially underpredicted the experimental inventory results, suggesting the possibility of tritium trapping in the bulk as playing an important role in tritium inventory.

MISTRAL can account for the following potentially important contributions to the overall tritium inventory: diffusive inventory, surface inventory, solubility inventory of reduced species based on Sievert's law, and pore inventory. Other potentially important inventory components are radiation effects which are difficult to characterize at this stage due to the limited data, and the general process of LiOT formation and solubility driven by the concentration of oxidized hydrogen species in the pore which, if high enough, could also result in LiOT precipitation (or separate phase formation). Here, solubility is taken in the larger sense whereby LiOT is considered as generally representative of the solute but not necessarily as the correct or only species [4].

Ideally, MISTRAL could be further refined to independently account for the surface and bulk inventories driven by the reduced and oxidized hydrogen species. However, in that case the individual activation energy of each of these surface processes would have to be specified which substantially increase the complexity of the computations. In addition, specific data on these different surface processes are lacking and the computations would have to rely on a large number of unknown parameters. It was deemed more reasonable to keep the MISTRAL focus on the reduced species surface effect and to approximate the effects of the oxidized species as part of an overall chemical trapping term which at steady state would be determined by the temperature and moisture partial pressure [4,6,7]. Thus, it is important to accurately estimate the amount of oxidized species found in the pore, which would also need to be included in the model. Note that the transient calculations are more difficult since they rely on characterization of rate constants for tritium trapping and detrapping in the bulk. This will be described in more detail in Section 4.3.

2. Model description

The model can be best described by the following tritium release scenario: A tritium atom is produced via a neutron reaction with a lithium atom in the grain and diffuses to the grain surface. Part of the diffusing tritium could get trapped in the bulk. At the surface tritium will either desorb to the pore or will go back to the bulk. There are six hydrogen species in the pore: T_2, HT, H_2, T_2O, HTO and H_2O. The tritium and protium atoms desorbed to the pore will either adsorb back to the surface or diffuse through the pore to the purge gas, where they are carried out of the solid breeder. Fig. 1 shows the different fluxes and pore species considered in the model.

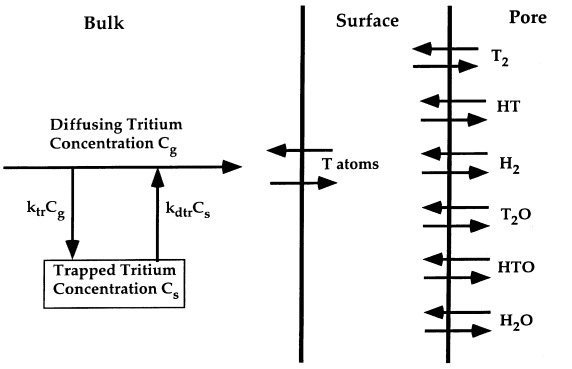

Fig. 1. Schematic diagram showing the bulk and surface fluxes, and the pore species assumed in the model.

From the above scenario, the following processes can be identified:

1. Diffusion of atomic tritium in the grain to the solid/gas interface.
2. Trapping and detrapping of the tritium in the bulk.
3. Surface processes consisting of bulk to surface migration, dissolution from the surface to the bulk, adsorption from the pore to the surface and desorption from the surface to the pore.
4. Diffusion of the gaseous species through the pore to the purge gas.

Different regions considered in the model are the grain, the surface and the pore. In the current model the capability to account for the grain boundary diffusion exists, but can be bypassed if desired. This was adopted in the subsequent analysis in light of the lack of data available on tritium transport in the grain boundary region.

A description of the calculations of the unit cell in the model can be found in Ref. [2]. The equations used in the model are summarized below. More details can be found in Refs. [2,8].

2.1. The grain

The grain is assumed to be spherical with radius r_g. Tritium is generated uniformly throughout the grain and is assumed to diffuse to the grain surface in accordance with Fick's law. The diffusing tritium flux would be affected by tritium trapping and detrapping in the bulk. The equations describing the diffusion and reactions of tritium are

$$\frac{\partial C_g(r,t)}{\partial t} = D_g(T)\left(\frac{\partial^2 C_g(r,t)}{\partial r^2} + \frac{2}{r}\frac{\partial C_g(r,t)}{\partial r}\right) + G(t) - \frac{\partial C_s(r,t)}{\partial t}, \tag{2}$$

$$\frac{\partial C_s(r,t)}{\partial t} = k_{tr}C_g(r,t) - k_{dtr}C_s(r,t), \tag{3}$$

where $C_g(r,t)$ is the mobile tritium concentration in the grain at position r and time t (at/m^3), $D_g(T)$ is the diffusion coefficient in the grain as a function of the temperature, T (assumed to be independent of C_g) (m^2/s), $G(t)$ is the uniform tritium generation rate (at/m^3 s), $C_s(r,t)$ and the trapped tritium concentration at position r and time t (at/m^3), k_{tr} is the reaction rate constant for tritium trapping in the bulk (s^{-1}), and k_{dtr} is the reaction rate constant for the tritium detrapping in the bulk (s^{-1}).

The boundary conditions used to solve the above equations are:

1. Symmetry at $r = 0$

$$\left(\frac{\partial C_g(r,t)}{\partial t}\right)_{r=0} = 0. \tag{4}$$

2. Conservation of tritium atoms: After a time increment Δt, the inventory of mobile tritium present in the grain is equal to the amount of mobile tritium that was present before Δt, plus the tritium generated in Δt, plus the tritium coming from the surface in Δt, plus the amount of detrapped tritium in Δt, minus the amount of tritium going to the surface in Δt, minus the amount of tritium trapped in Δt.

$$\int_{v_g} C_g(r,t+\Delta t)\,dv = I_{old} + G(t)\Delta t - \mathscr{R}_\beta A_g \Delta t + \mathscr{R}_{diss} A_{s/g}\Delta t + I_{old}(trap) - \int_{v_g} C_s(r,t+\Delta t)\,dv, \tag{5}$$

where I_{old} is the mobile tritium inventory inside the grain at time t (atoms), I_{old} (trap) is the trapped tritium inventory inside the grain at time t (atoms), v_g is the grain volume (m^3), $\mathscr{R}_\beta$ is the flux of tritium atoms going to the surface from the bulk (at/m^2 s), A_g is the grain surface area (m^2), $\mathscr{R}_{diss}$ is the flux of atoms going to the bulk from the surface (at/m^2 s), and $A_{s/g}$ is the surface area associated with one grain (m^2).

Eqs. (4) and (5) are used together with the diffusion equation (Eq. (2)) to obtain a set of linear equations that are solved numerically to obtain the diffusive inventory, C_g, at each time step. Since Eq. (3) is a rate equation, no boundary conditions are required to solve it.

2.2. The surface

There are four surface fluxes coming in and out of the surface. Fig. 2 shows the different fluxes entering and leaving the surface.

1. A flux of tritium atoms entering the surface from the bulk side

$$\mathscr{R}_\beta = k_\beta C_g(r_g, t)\,(1-\theta), \tag{6}$$

$$k_\beta(T) = \beta_o\ \exp(-E_\beta/RT). \tag{7}$$

β_o can be estimated based on the vibration frequency of the atoms. According to Pick and Sonnenberg [9]

$$\beta_o = \frac{10^{13}}{\sqrt{N_s}}, \tag{8}$$

where $C_g(r_g,t)$ is the tritium concentration just beneath the surface at time t (at/m^3), θ is the total surface coverage, E_β is the activation energy for adsorption from the bulk (J/mol), R is the universal gas constant (J/mol K), and N_s is the number of surface sites (sites/m^2).

2. A flux of molecules of species (i) (tritium or protium containing molecule) entering the surface from the pore side (the adsorption flux)

$$\mathscr{R}^{(i)}_{ads} = k^{(i)}_{ads}(T,\theta)C^{(i)}_p(z,t)(1-\theta)^m, \tag{9}$$

$k^{(i)}_{ads}(T,\theta)$ is calculated from Ref. [10]

$$k^{(i)}_{ads}(T,\theta) = \frac{\sigma z_{adj}}{\sqrt{8\times10^{-3}\pi}}\sqrt{\frac{RT}{M^{(i)}}}\exp(-mE_{ads}(\theta)/RT), \tag{10}$$

where $E_{ads}(\theta)$ is the adsorption activation energy (J/mol), σ is the condensation factor ($\sigma \sim 0.4$ [2]), z_{adj} is the number of adjacent sites ($=4$ [2]), $M^{(i)}$ is the molecular weight of species (i) (g/mol), $m=1$ for first order adsorption and $=2$ for second order adsorption, and $C^{(i)}_p(z,t)$ is the concentration of gaseous species (i) in the pore at position z and time t (molecules/m^3).

3. A flux of molecules of species (i) leaving the surface to the pore (the desorption flux) [2]

$$\mathscr{R}^{(i)}_{des} = k^{(i)}_{des}(T,\theta)\theta_j\theta_k, \tag{11}$$

$$k_{des}(T,\theta) = \frac{N_s z_{adj} RT}{N_{avo}h}\ \exp(-mE_{des}(\theta)/RT), \tag{12}$$

where $E_{des}(\theta)$ is the desorption activation energy (J/mol), N_{avo} is the Avogadro's number (particles/mol), h is Planck's constant (j,s), θ_k, θ_j are the surface coverages of atomic species k and j that constitute molecule (i), and $m=1$ for first order desorption, $=2$ for second order desorption.

For first order desorption, only θ_T is used in Eq. (11) for tritium desorption.

4. A flux of tritium atoms leaving the surface to the bulk (the dissolution flux)

$$\mathscr{R}_{diss} = k_{diss}(T)\theta_T, \tag{13}$$

where, by analogy to k_{des}, k_{diss} can be expressed by

$$k_{diss}(T) = \frac{N_s z_{adj} RT}{N_{avo}h}\ \exp(-E_{diss}/RT). \tag{14}$$

E_{diss} is the activation energy of dissolution (J/mol) and θ_T is the tritium surface coverage.

The surface coverage of species (j) ($=$tritium or protium) is obtained by solving the coverage rate equation for this species

$$\frac{d(N_s\theta_j)}{dt} = \mathscr{R}_\beta + \sum_i n\mathscr{R}^{(i)}_{ads} - \sum_i n\mathscr{R}^{(i)}_{des} - \mathscr{R}_{diss}, \tag{15}$$

where $\mathscr{R}^{(i)}$ is the flux of molecules (i) containing atomic species (j), and n is the number of (j) atoms in an (i) molecule. Note that for protium, $\mathscr{R}_\beta$ and $\mathscr{R}_{diss}$ equal zero. The total surface inventory, θ, is equal to the summation of the surface coverages of all the atomic species present.

The activation energies of the four fluxes are related through the heat of adsorption, Q, as well as the activation energy of solution, E_s:

$$Q = E_{des} - E_{ads}, \tag{16}$$

$$E_s = (E_{diss} - E_\beta) - (E_{des} - E_{ads}). \tag{17}$$

Fig. 3 shows a schematic of the different activation energies. Both protium and tritium surface fluxes are considered. Protium would also migrate to and diffuse in the bulk where it could affect the formation, solubility

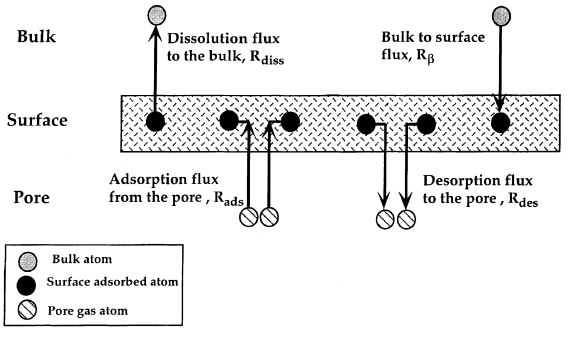

Fig. 2. Schematic of the fluxes entering and leaving the surface.

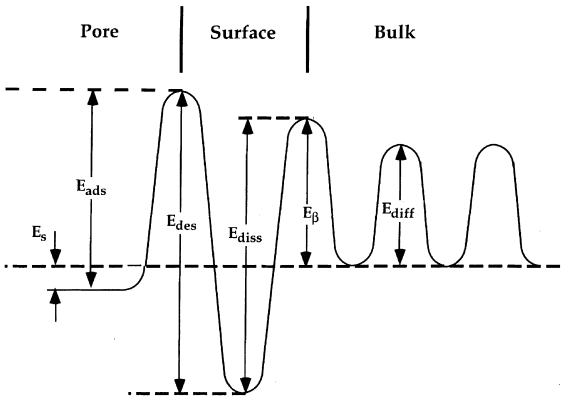

Fig. 3. Potential energy diagram for atomic and molecular hydrogen at the surface.

and possible precipitation of LiOH/LiOT. However, inclusion of protium transport and trapping in the bulk would substantially add to the model complexity and was omitted at this stage under the assumption that tritium diffusion in the bulk could be independently calculated and that the tritium bulk trapping and detrapping fluxes would mostly be dependent on the tritium concentrations in the bulk.

2.3. The pore

The pore is modeled as a straight cylinder of length z_{ip}. Pore diffusion is assumed to be one-dimensional. For gas species (i)

$$\frac{\partial C_p^{(i)}(z,t)}{\partial t} = \frac{\partial}{\partial z}\left(D_{peff}^{(i)} \frac{\partial C_p^{(i)}(z,t)}{\partial z}\right) + G_p^{(i)}(z,t), \tag{18}$$

or

$$\frac{\partial C_p^{(i)}(z,t)}{\partial t} = \frac{\partial D_{peff}^{(i)}}{\partial z}\frac{\partial C_p^{(i)}(z,t)}{\partial z} + \left(D_{peff}^{(i)}(T)\frac{\partial^2 C_p^{(i)}(z,t)}{\partial z^2}\right) + G_p^{(i)}(z,t), \tag{19}$$

where $D_{peff}^{(i)}(T)$ is the effective pore diffusion coefficient for species (i) as a function of temperature (T) (m^2/s) and $G_{p(z,t)}^{(i)}$ is the effective volumetric source term for species (i) at position z and time t based on the corresponding net desorption rate (molecules/m^3 s).

The capability to account for the temperature change along the interconnected porosity is included to model cases where large temperature gradients can result over the ceramic breeder, such in Be/ceramic breeder blankets. Due to the temperature changing with position, D_{peff} will also be a function of position. This improves on the original model which neglects the first term on the RHS of Eq. (19).

The boundary conditions used for solving the pore diffusion equation are [2]:

1. Zero concentration gradient for each species (i) at the beginning of the interconnected pore, $z = 0$:

$$\left(\partial C_p^{(i)}\frac{(z,t)}{\partial z}\right)_{z=0} = 0. \tag{20}$$

2. Given concentration for each species (i) at the end of the interconnected pore system:

$$C_{p(z_{ip},t)}^{(i)} = C_{purge}^{(i)}. \tag{21}$$

There are three regimes possible for the calculation of $D_{peff}(T)$ depending on the pressure, temperature and mass of the diffusion atoms. These regimes are:

1. Ordinary diffusion in which molecular collisions dominate the diffusion process.
2. Knudsen diffusion in which collisions of the diffusing molecules with the porous solid dominate the diffusion process, and
3. A transition region between ordinary and Knudsen diffusion.

Details on the calculations of the pore diffusion coefficient and the pore source terms are found in Federici et al. [2].

In order to calculate the tritium release accurately, all the different gaseous species and compounds in the pore should be accounted for at each step. This is a very complicated task, since there are too many unknowns and insufficient experimental data. Consequently, it is assumed that there are only six gaseous species: H_2, T_2, HT, H_2O, T_2O and HTO, in the pore. In other words, all the oxygen is assumed to be in combination with protium and/or tritium (see Ref. [11]). Therefore,

$$N_O = N_{HTO} + N_{T_2O} + N_{H_2O}, \tag{22}$$

where N_O is the total number of oxygen atoms in the pore, N_{HTO} is the total number of HTO molecules in the pore, N_{H2O} is the total number of H_2O molecules in the pore, and N_{T2O} is the total number of T_2O molecules in the pore.

Calculations of the concentrations in the pore are based on the simplifying assumption that at any given pore location the ratio of protium to tritium atoms in oxidized form is equal to the ratio of the total number of protium to tritium atoms, i.e.,

$$\frac{N_{HTO} + 2N_{H_2O}}{N_{HTO} + 2N_{T_2O}} = \frac{N_H}{N_T}. \tag{23}$$

N_H is the total number of protium atoms in the pore and N_T, the total number of tritium atoms in the pore

From those two assumptions, the concentrations of different species in the pore can be calculated with the aid of the following equations:

$$N_{HT} + 2N_{H_2} = N_H - N_{HTO} - 2N_{H_2O}, \tag{24}$$

$$N_{HT} + 2N_{T_2} = N_T - N_{HTO} - 2N_{T_2O}, \tag{25}$$

$$\frac{(N_{HT})^2}{N_{T_2} + N_{H_2}} = K_r, \tag{26}$$

$$\frac{(N_{HTO})^2}{N_{T_2O} + N_{H_2O}} = K_o, \tag{27}$$

where N_{H2} is the number of N_{H_2} molecules in the pore, N_{T2} is the number of N_{T_2} molecules in the pore, N_{HT} is the number of N_{HT} molecules in the pore, K_r is the equilibrium constant for the reduced species, and K_o is the equilibrium constant for the oxidized species.

2.4. Summary of the assumptions in the upgraded model

The following assumptions were made in the model:

1. The solid breeder grains are assumed to be spherical for ease of calculation.
2. Uniform generation of tritium throughout the solid breeder grain.
3. At this stage, only tritium is modeled in the bulk assuming that tritium diffusion can be estimated independently of protium and that the tritium trapping and detrapping fluxes can be estimated solely from the bulk tritium concentrations.
4. No radiation induced effects within the grain.
5. The grain boundaries are assumed to be paths where diffusion is fast, and are thus neglected.
6. The amount of oxygen desorbing to the pore is equal to half the amount of desorbing tritium.
7. The pores are represented as interconnected cylindrical capillaries.
8. All oxygen in the pore is assumed to be in combination with hydrogen species.
9. The ratio of protium to tritium atoms in oxidized form is equal to the ratio of the total number of protium to tritium atoms.
10. No tritium retention within the pore because of sintering and consequent partial or complete closure of the transport paths.
11. Local chemical equilibrium is assumed in the pore network.

3. Validation of the model: comparison with experimental results

A large number of laboratory and in-reactor tests have been conducted to determine the tritium retention and release characteristics of lithium oxide as a function of microstructure, purge gas flow rate and chemical composition, temperature, generation rate and burnup. Computer modeling of the fundamental retention and release mechanisms is needed to extrapolate the results of these experiments to design applications. A primary objective of in situ experiments is to determine viable operating parameters for solid breeder blankets and the associated tritium inventories. However, because the results of the experiment reflect the tritium recovery rates for the total system, this fact must be considered when interpreting the results for tritium release from the solid breeder specimen.

The data produced from in-reactor tests can be divided into three types [12]. The first type is the tritium inventory data at the sample end of life. This type of data is extremely useful in that a very small error or uncertainty is associated with it. The major uncertainty in using such data for model validation is associated with changes in breeder microstructure which may have occured during irradiation as well as the uncertainty of whether reactor shutdown occurred after steady state has been reached. The second type of data is the change of inventory associated with changes in the operating conditions. This type of data can be obtained by integrating the tritium concentration in the purge gas. There are four major uncertainties associated with such data. One uncertainty is associated with possible changes to the tritium detection system calibration and baseline due to changes in operating conditions. The second is the lack of knowledge of the changes in the lines connecting the sample to the detection system. The third is the uncertainty in the tritium generation rate, which forms a baseline for the calculations. The fourth is the uncertainty of whether steady state conditions have been reached prior to the transient.

The third type of information that can be obtained from an in situ experiment is the time history of the tritium release rate during the transient in operating condition. In using this information for model validation, the same uncertainties associated with deriving an inventory change are involved in deriving a release rate. In addition, there is the uncertainty of the degree to which the tritium processing equipment and the overall time response of the system influence the time history of the signal.

Based on the above argument, it can be concluded that the most reliable source of information would come from the end of life inventory, followed by the change in inventory data due to the change in operating conditions. The least reliable data would be obtained from the time history of the tritium release rate during a transient.

The analysis in this paper is mainly focused on the BEATRIX-II experiment, since it provides some of the latest experimental results for Li_2O. In addition, experimental results from MOZART, CRITIC-I and EXOTIC-2 experiments are used for validation of inventory calculations.

The analysis plan was to match the changes in inventory from BEATRIX-II with the calculated values, by changing the input parameters within acceptable ranges. After matching the inventory changes, the experimental end-of-life inventories would be estimated based on the calibrated input data for samples from BEATRIX-II and other experiments. These would then be compared to the BEATRIX-II end-of-life inventory measurements which became later available. Finally, the tritium release histories for given transients would be calculated and compared to the experimental results from BEATRIX-II.

3.1. Change-in-inventory calculations

In order to analyze experimental data, or do calculations in general, a set of input properties and parameters have to be used. These properties include the

sample characteristics, which should be given in the experiment, as well as the material properties which should be available from the database and from specific experiments done to obtain them. Unfortunately, there are many data missing for lithium oxide, and, thus, parametric studies have to be made in order to obtain the set of input data that would best reproduce the experimental results.

Based on the analysis by Badawi et al. [13], the activation energies that will affect the tritium surface and surface-driven bulk inventories in Li_2O are: the activation energy of adsorption, E_{ads}, the activation energy of solution, E_s, the heat of adsorption, Q, and the bulk-to-surface-flux activation energy, E_β. Other parameters that can affect the steady state inventories are: the pore diffusion, the pre-exponentials of the surface fluxes, and the bulk diffusion coefficient.

LiOT formation and solubility could contribute appreciably to the tritium inventory in experiments such as BEATRIX-II. However, the typical moisture pressure observed experimentally would be too low for LiOT precipitation to occur based on the results of Gregory and Mohr [6] and Tetenbaum and Johnson [14]. Moreover, the kinetics of LiOT formation and solubility are not well characterized in terms of rate equations and it was decided for this study to assume an initial detrapping rate constant based on the thermal decomposition of LiOT and to vary it in order to observe its effects, as will be described in more detail in Section 4.3. The trapping rate constant would then be analogous to the formation of LiOT(l,s) whose equilibrium constant was based on the data of Refs. [6] and [14].

The bulk diffusion coefficient has been well characterized from past experiments (see Ref. [12]) and its value was also kept constant. The value of the desorption activation energy, E_{des}, was obtained from Ref. [15]. Because of lack of data, E_{des} was assumed to be independent of the surface coverage. E_{ads} is not known for Li_2O. However, it is known to be small for $LiAlO_2$. Since the value of E_{ads} will not affect the tritium inventory except at high values, as shown from the parametric study presented in Ref. [13], it was assumed to be 30 kJ/mol in the present analysis. Due to the fact that pore diffusion will be affected by pore size distribution, a reference value of 0.1 of the calculated pore diffusion coefficient was used. This value is known to be reasonable from past experiences of Federici et al. [16]. Table 1 shows the reference values of parameters used in the analysis of experimental data.

The range in which the parameters in Table 1 were changed was chosen according to the uncertainties associated with each parameter. Experiments by Katsuta [17] using reduced protium and deuterium with Li_2O found the activation energy of solution, E_s, to be between 16 and 19 kJ/mol, whereas experiments by O'hira and Kudo [18,19] with moisture and Li_2O found it to be 24–25 kJ/mol. Therefore, E_s was changed in the range 15–30 kJ/mol. The range for changing the heat of adsorption was based on the surface coverage. Any value of Q that produced a surface coverage of more than 0.6 was excluded from the results, since such a high value was assumed to be improbable. Since the values of the pre-exponentials of the surface fluxes, as described by Trapnell et al. [20], were based on the vibration frequency, an uncertainty of about one order of magnitude seemed reasonable. Finally, the pore diffusion coefficient was changed between 1, which corresponds to the calculated value that neglects the effect of pore size distribution, to 0.001, which seems extremely improbable.

For the change-in-inventory calculations, the experimental data from BEATRIX-II Phase I ring sample were used. Table 2 shows the Phase I ring sample characteristics.

The first case considered in the analysis was the case of a change in temperature between 550°C and 650°C. The experimental change of inventory, ΔI, associated

Table 1
Reference values of parameters used in the analysis of experimental data

Grain diffusion coefficient, D_g	
$D_g = D_o(-E_{diff}/RT)$	
Pre-exponential (m^2/s), D_o	4.033×10^{-6} [12]
Activation energy (kJ/mol), E_{diff}	95.1 [12]
Reference values of activation energies	
Adsorption activation energy, E_{ads} (kJ/mol)	30
Desorption activation energy, E_{des} (kJ/mol)	140
Heat of adsorption, Q (kJ/mol)	110
Activation energy of solution, E_s (kJ/mol)	20
Bulk-to-surface-activation energy, E_β	$E_\beta = E_{diff} + E_{ads}$
Dissolution activation energy, E_{diss}	$E_{diss} = E_s + E_\beta + E_{des} - E_{ads}$
Pore diffusion coefficient multiple, f_{Dp}	0.1
Equilibrium constant for LiOT formation Eq. (Eq. (1)), K_{equi}	Refs. [6,13]

Table 2
BEATRIX-II Phase I ring sample characteristics [5]

Length (m)	0.089
Outer diameter (m)	0.01843
Inner diameter (m)	0.01514
Weight (kg)	1.195×10^{-2}
Porosity (%)	20.7
Purge gas pressure (Pa)	$\approx 2.5 \times 10^{5}$
Grain radius (m)	2.75×10^{-6}
Surface area (m^2/kg)	60

with this temperature change was about 50 ± 10 mCi. When the reference parameters in Table 1 were used without including chemical trapping, the tritium inventory changed from 2.7 mCi at 550°C to 2.4 mCi at 650°C, giving a change in inventory of 0.3 mCi, which is off by a factor of more than 150. When chemical trapping was included, the inventory changed from 160 mCi at 550°C to 65 mCi at 650°C. Although these inventory values produce a change in inventory that is different from the experimental value ($\Delta I = 95$ mCi calculated vs. 50 mCi experimental) this value is much closer to the experiment than that calculated without including chemical trapping.

In order to obtain a better estimate of ΔI, each of the reference values in Table 1 was changed within a reasonable range and the effect on the inventory was calculated in each case. The effect of changing the different parameters on the different components of the inventory are discussed in detail in Ref. [8] and summarized below.

Fig. 4 shows the effect of the activation energy of solution on the change in inventory for 0.1% H_2 and temperature change of 550–650°C. When trapping was excluded, most of the inventory was found on the surface of the grain. This makes the total inventory independent of the activation energy of solution. When trapping based on LiOT formation was included, most of the tritium inventory was found in the bulk with about 10% on the surface. This gives an exponential dependence of the inventory on E_s. In this case, the experimental value of ΔI can be achieved by increasing E_s slightly.

The effect of the heat of adsorption on the change in inventory was also investigated. Increasing Q increases the surface inventory but not the bulk inventory. However, since the latter constitutes most of the tritium inventory in the sample, the total inventory is not affected much by changing Q, except for very high values of Q.

The effect of the pore diffusion on the change in tritium inventory was investigated by multiplying the pore diffusion coefficient by a factor, f_{D_p}, in order to account for the effect of the different pore sizes present in the sample [16]. As f_{D_p} is increased, the tritium concentration in the pore decreases, which results in decreases of

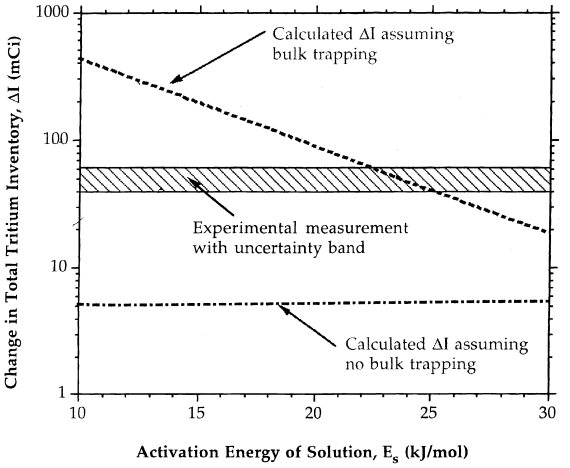

Fig. 4. Effect of the activation energy of solution on the change in tritium inventory for 0.1% H_2 and 550°C–650°C temperature change.

both the bulk and surface inventories. However, no realistic value of f_{D_p} was found that could reproduce the experimental change of inventory for the set of reference parameters.

The effect of the surface fluxes on the change in tritium inventory was examined by changing the preexponential of each flux between 0.1 and 10 times the reference value. The total inventory was found to change with all of the surface fluxes. The bulk inventory was found to increase exponentially with increasing desorption flux and/or dissolution flux. The total inventory was also found to increase almost exponentially with increasing adsorption flux due to the increase in tritium surface coverage and corresponding increase in the dissolution flux. The experimental value of ΔI could be obtained by changing either the adsorption flux or the desorption flux to about 0.2 of its reference value, or by changing the bulk-to-surface flux by a factor of 2, but only when including chemical trapping in the assumed form of LiOT formation. Otherwise, the experimental value of ΔI could not be reproduced even when changing the surface fluxes by more than two orders of magnitude.

From the above analysis, it appears that some form of bulk trapping (assumed here as LiOT formation and solubility) plays an important role in the determination of the tritium inventory. The analysis suggests that the parameters that can reproduce the experimental change in inventory in this case are:

1. Using an activation energy of solution of about 23 kJ/mol.
2. Using a desorption flux pre-exponential less than the reference value by a factor of 0.2.
3. Using an adsorption flux pre-exponential less than the reference value by a factor of 0.2.

4. Using a bulk-to-surface pre-exponential more than the reference value by a factor of 2.

It seems more reasonable to change the activation energy of solution to $E_s = 23$ kJ/mol, which is within the range of values experimentally determined in O'hira et al. [18] and Kudo et al. [19]. By using $E_s = 23$ kJ/mol, the calculated change in inventory was found to be ≈60 mCi, which is within the range of uncertainties in the experimental data.

In order to further explore the adequacy of MISTRAL in estimating the change in inventory in BEATRIX-II, another set of data concerning a series of temperature changes was examined. The predicted inventory changes were calculated based on the reference parameters listed in Table 1 and with $E_s = 23$ kJ/mol. Large uncertainties were associated with the determination of the steady state baseline for the experimental set of data, as discussed by Billone [12]. Since each transient only leads to 10% change in the tritium release, choosing the baseline is crucial in the calculation of the change in inventory. The first case involved a temperature change from 638°C to 600°C. The change in inventory was 28 ± 54 mCi. The calculated inventory changes from 47 mCi at 638°C to 64 mCi at 600°C, with a difference of 17 mCi. The second temperature change was from 600°C to 550°C. The calculated inventory changed from 64 to 102 mCi with a difference in inventory of 38 mCi. The experimental value was 36 ± 27 mCi. The third temperature change was from 550°C to 597°C. The calculated inventory changed from 102 to 66 mCi. The calculated loss in inventory was 36 mCi as compared to the experimental value of 24 ± 19 mCi.

BEATRIX-II involved the examination on the effect of the tritium release of transients of temperature, purge gas composition and flow rates, burnup, and power. Since the effect of radiation induced trapping was not included in the model, it is not possible to investigate the effect of burnup. Thus it was excluded from the analysis.

The effect of purge gas composition was examined in BEATRIX-II by varying the amount of H_2 in the purge between 0% and 0.1%. Fig. 5 shows the tritium release history with the change in the amount of protium in the purge. From the figure it can be seen that when the protium in the purge was switched off and pure helium was used for purging the sample, the steady state was not reached even after 90 h. This strongly indicates that the tritium is not being retained in the sample, but in the stainless steel lines.

Assuming that steady state was reached at the beginning and end of the H_2 change series, the change in the tritium inventory was calculated in each case. Calculation of the area under the curve shows that there is a gain of 12 Ci for the change from He + 0.1% H_2 to pure helium, followed by a release of 2.5 Ci for the change of pure helium to He + 0.01% H_2 and a release of 2.65 Ci for the change from He + 0.01% H_2 back to He + 0.1% H_2. This shows there is a difference of ≈6.8 Ci between the start and the end of this transition series. Since the series started and ended with the same conditions, that is 650°C and 0.1% H_2 in the purge, this huge amount of tritium has to be either trapped in the sample or in the lines. However, the reactor shut down occurred at the same conditions as the end of this transient series, namely 650°C and He + 0.1% H_2 in the purge. The tritium inventory at the sample's end of life was found to be only 50 mCi. This strongly indicates that all of this tritium was actually deposited on the stainless steel lines. Therefore, this set of data is unreliable and cannot be reproduced using MISTRAL, which does not account for the effect of the lines connecting the sample to the tritium monitoring system.

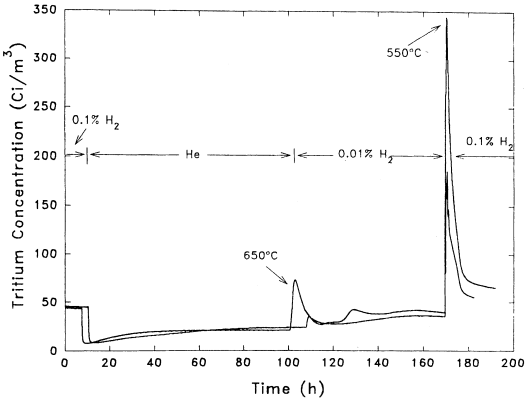

Fig. 5. Measured tritium concentration during purge gas composition change change series between pure helium and He + 0.1% H_2 [5].

However, for completeness, the changes of inventory predicted by MISTRAL for these cases of purge gas composition changes were also calculated using the data in Table 1, with $E_s = 23$ kJ/mol. These are included in Table 3 which shows a summary of the results of all the cases studied in the change of inventory analysis.

3.2. End-of-life calculations

The reactor shutdown in BEATRIX-II occurred at 640°C while the sample was purged with He + 0.1% H_2 for about half a day after shutdown then changed to pure helium. The temperature decreased from 640°C to 335°C in 20 min then stayed at 335°C for about 8 h before decreasing again to 300°C. Although the tritium release profile with time was not measured, the tritium inventory at the end of life was measure and was found to be 50 mCi [21].

Both the data shown in Tables 1 and 2 were used in order to calculate the end of life inventory. However, the activation energy of solution was replaced by 23 kJ/mol

Table 3
MISTRAL predictions of the change of inventory of the BEATRIX-II Phase I ring sample (Note that $\triangle I$ experiment for purge gas composition changes carries huge uncertainties due to the effect of the lines as explained in the text)

Temperature (°C)	Purge gas composition	$\triangle I$ Model (mCi)	$\triangle I$ Experiment (mCi)
550 → 650	He + 0.1% H_2	− 60	− 48 ± 10
650 → 550	He + 0.1% H_2	+ 60	+ 50 ± 10
638 → 600	He + 0.1% H_2	+ 17	+ 28 ± 54
600 → 550	He + 0.1% H_2	+ 38	+ 36 ± 27
550 → 597	He + 0.1% H_2	− 36	− 24 ± 19
640	He + 0.1% H_2 → He	+ 903	(+ 12 ± 10) × 10^3
640	He → He + 0.01% H_2	− 825	(− 2.5 ± 10) × 10^3
640	He + 0.01% H_2 → He + 0.1% H_2	− 78	(− 2.65 ± 10) × 10^3

instead of 20 kJ/mol. In this case the inventory was found to be ≈46 mCi, with most of it in the bulk. If chemical trapping is neglected, the calculated tritium inventory is only about 1 mCi, with the majority on the surface (see Ref. [22]).

For verification, data from MOZART, EXOTIC-2, and CRITIC-I experiments were used for comparison with the MISTRAL calculations. Table 4 shows the sample characteristics and end of life conditions in each experiment.

The steady state inventory for the MOZART sample was calculated using the end-of-life conditions: 350°C and He + 0.1% H_2 purge gas, in addition to the data in Table 5. The calculated inventory in this case was 176 mCi, which is higher than the experimentally determined value of 110 mCi (note that this data point is of lower value in a sense since the inventory was not directly measured but rather estimated from the experimental results). Note that the assumed equilibrium constant for the formation of LiOT, estimated here from Gregory and Mohr's data [6], is a key factor in determining the inventory especially at low temperatures, and could also explain some of this discrepancy.

The inventory for the EXOTIC-2 high temperature sample was calculated using steady state conditions of 610°C and He + 0.1% H_2 purge gas. The resulting inventory was 0.83 mCi for the whole sample, or 0.46 mCi/g compared to <0.5 mCi/g from the experiment. Note, however, that the surface area in this case was assumed to be 50 m^2/kg; if it were assumed higher, it would produce higher inventory.

The inventory for the CRITIC-I sample end of life was calculated using steady state conditions of 600°C and He + 0.1% H_2 purge gas. The calculated inventory was found to be 182.5 mCi per pellet of 5.5 gm. This means that for the whole sample, the inventory is equal to 3.47 Ci which is almost 3.5 times higher than the experimental value. Note that this sample was a high density sample with 14 ± 6% porosity. This large uncertainty in the porosity can lead to large uncertainties in the calculated inventory.

3.3. Transient analysis

The transient cases that were considered in the analysis were temperature transients. These cases were chosen in order to minimize the effect of the lines on the measured tritium release, since the temperature changes affect mostly the sample, whereas the purge gas changes affect the sample as well as the lines.

Table 4
Li_2O samples characteristics and end of life conditions for MOZART [23], EXOTIC-2 [24], and CRITIC-I [25]

	MOZART	EXOTIC-2	CRITIC-I
Sample volume (m^3)	1.5×10^{-6}	1.1×10^{-6}	3.6×10^{-6}
Sample weight (kg)	2.28×10^{-3}	1.8×10^{-3}	0.103
Porosity (%)	20	20	14 ± 6
Grain radius (m)	8×10^{-6}	(2.5–5.5) × 10^{-5}	(2.5–3) × 10^{-5}
Surface area (m^2/kg)	50	50 (assumed)	100
Purge gas pressure (Pa)	≈ 1.6×10^6	–	10^5
Purge gas flow rate (L/h)	2.4792	–	6
Temperature at shutdown (°C)	350	610	600
H_2 in Purge gas (%)	0.1	0.1	0.01
End-of-life inventory			
Experimental (mCi)	110	0.9	10^3
Calculated (mCi)	176	0.83	3.47×10^3

Table 5
BEATRIX-II Phase II ring sample characteristics [21]

Length (m)	0.089
Outer diameter (m)	0.0185
Inner diameter (m)	0.01514
Weight (kg)	8.103×10^{-2}
Porosity (%)	12.7
Grain radius (m)	2.2×10^{-5}

The first case was a temperature decrease from 642°C to 557°C. The second was a temperatures increase from 557°C to 642°C. Both cases were purged with He + 0.1% H_2. Fig. 6 shows the temperature and tritium release histories of both cases.

The data in Tables 1 and 2 were used with $E_s = 23$ kJ/mol. In addition, for transient cases, k_{tr} and k_{dtr} from Eq. (3) need to be characterized. Under the general assumption of LiOT formation and solubility, and precipitation under high enough moisture pressure as trapping mechanisms, and in the absence of other fundamental reaction rate data, k_{dtr} was assumed analogous to the decomposition rate constant for LiOT as an initial step. Using Li_2O irradiated under a fluence of 3.6×10^{16} n/cm^2, Kudo et al. [26] found the decomposition rate constant, k_{dsn}, to be

$$k_{dsn}(s^{-1}) = 1.6 \times 10^3 \exp(-7.86 \times 10^4/RT), \quad (28)$$

where R is the universal gas constant in J/mol-K and T the temperature in K.

The rate constant in Eq. (28) is lower than that for the decomposition of pure unirradiated LiOH from Ref. [27], which suggests that the LiOH decomposition rate could be dependent on the exact material composition and on experimental conditions. At 650°C, the temperature at which BEATRIX-II was operating, the rate constant from Eq. (28) is about two orders of magnitude lower than that from Ref. [27].

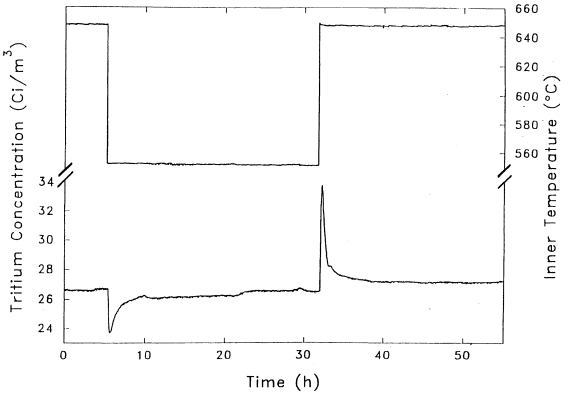

Fig. 6. Measured temperature and tritium concentration histories for the temperature transients considered in the analysis [5].

The above discussion indicates that even if assuming LiOT precipitation under BEATRIX-II conditions the LiOT decomposition rate constant could be different from that obtained from Eq. (28) since the parameters of the BEATRIX-II experiments are different from those used in deriving Eq. (28). For example, the fluence in the case of BEATRIX-II was 3.8×10^{22} n/cm^2 [5], which is six orders of magnitude higher than in the experiment by Kudo [26].

Eq. (28) was then assumed as the initial value for k_{dtr} in Eq. (3) and a parametric analysis was carried out to observe the effect on the tritium release of varying k_{dtr} between 1 and 0.01 times the reference value of Eq. (28). The chemical trapping rate, k_{tr}, would also be changed in each case in accordance with Eq. (29) based on the equilibrium constant, K_{equi}, for the reaction shown by Eq. (1). K_{equi} was based on the data from Refs. [6] and [14]. The LiOT formation rate constant was obtained from

$$k_{tr} = K_{equi} \times k_{dtr}. \quad (29)$$

The following key parameters were changed from their reference values (Table 1 and Eq. (28)) to determine how they would affect the tritium release under 642–557°C temperature transient:

Pore diffusion coefficient: As the pore diffusion coefficient is decreased, the drop in the tritium release due to the transient temperature change increases and the time to reach steady state increases. This is because of the increase in the change in tritium inventory in these cases. However, for values of f_{D_p} between 0.001 and 1, the measured tritium release drop could not be reproduced. The closest reproduction was obtained with $f_{D_p} = 0.1 - 1$ for which the normalized tritium release drop was 0.696 compared to the experimental value of 0.884.

Heat of adsorption: As the heat of adsorption is decreased, the drop in the tritium release becomes more pronounced since a decrease in the heat of adsorption makes it easier for the tritium to leave the surface, and hence the sample. However, no significant effect on the change in tritium inventory was observed.

Bulk-to-surface flux: As this flux is increased the drop in the tritium release decreases. For $f_\beta = 10$, the normalized drop was 0.791 as compared to the experimental value of 0.884. However, this result is misleading because the absolute change in inventory for this case is low, about 5 mCi, which is about one order of magnitude less than the experimental value. Also, the tritium inventory at 642°C in this case is less than 6 mCi, which is much less than the end-of-life inventory (50 mCi) that was obtained under similar conditions.

Desorption and dissolution fluxes: Increasing these fluxes produce competing effects, the dissolution flux tending to increase the inventory and the desorption flux tending to decrease the inventory. As a result, the net effect is not very clear However, in all the cases, the

experimental tritium release profile could not be reproduced.

Adsorption flux: Increasing the adsorption flux seems to increase the tritium release drop to about 0.375 (normalized) for $f_{ads} = 10$, which is much less than the experimental value. Decreasing the adsorption flux, however, decreases the tritium release drop to 0.76 (normalized) for $f_{ads} = 0.1$, a value close to the experimental value (0.884, normalized). However, in this case, the tritium release returns to steady state in less than 1.5 h, which is much faster than the experiment.

These results indicate that the measured tritium release profile cannot be reproduced by changing any of the above parameters. The fact that most of the inventory is present in the bulk leads to the conclusion that a process governing bulk tritium transport needs to be changed in order to slow down the tritium transport inside the grains. Since diffusion is so fast in Li_2O, this process must be linked to bulk trapping represented here by LiOT formation and solubility.

Following the earlier discussion, k_{dtr} was varied by factors of 0.01 to 1 from the initial value of k_{dsn} (Eq. (28)). Decreasing the rate constant was observed to decrease the drop in the tritium release and increase the time required to reach steady state after a transient. For $k_{dtr} = 0.01\ k_{dsn}$, the drop was equal to 0.809 (normalized) which is close to the experimental value of 0.884 (normalized).

For the second temperature transient involving a temperature increase from 557°C to 642°C (see Fig. 6), decreasing k_{dtr} led to a smaller peak and a longer time to reach steady state. Note that the total change in inventory is the same in all the cases since changing the assumed LiOT formation and decomposition rate constants by the same factor does not change the steady state inventories. Using $k_{dtr} = 0.01$ of kdsn produced a peak of 1.37 (normalized), which is close to the experimental peak of 1.25 (normalized).

Based on the above analysis, the values that are recommended to reproduce both inventory change and the tritium release results of BEATRIX-II are those in Tables 1 and 2, together with an activation energy of solution of 23 kJ/mol and $k_{dtr} = 0.01\ k_{dsn}$ of Eq. (28). Using these data, the calculated tritium release history for the temperature transient series is shown in Fig. 7. The shifts that are found in the peaks from the experimental values could be explained by the fact that it takes 15 min for the tritium to reach the monitors from the samples. The difference between the calculated and measured tritium release in the time between the transient is within the uncertainty in the determination of the release baseline.

The change in the tritium inventory for the temperature transients is shown in Fig. 8. Most of the tritium is found in the bulk. Since the experiment did not measure the tritium inventory profile, the calculated inventory

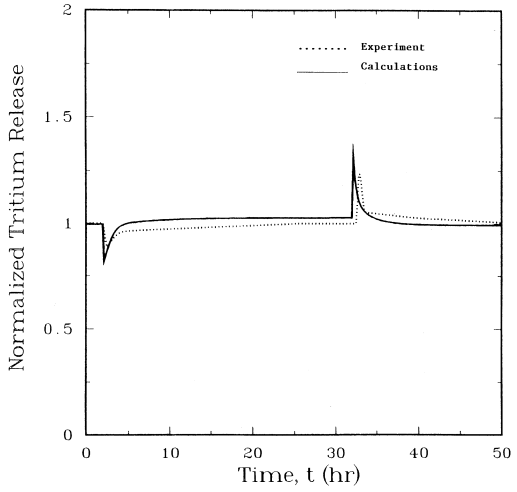

Fig. 7. The normalized tritium release history for a change in the sample temperature of 642–557–642°C.

could not be compared with the experiment. However, from the change in inventory analysis, the change in inventory between steady states is close to those of the experimental values.

In order to further validate the modeling results, the latest released results for a ring specimen from the BEATRIX-II Phase II experiment were analyzed. The selected specimen is a high density, large-grained Li_2O sample whose characteristics are shown in Table 5.

The first case considered was a temperature transient between 640°C and 550°C and 0.1% H_2 in the purge gas. Fig. 9 shows the maximum temperature history for the

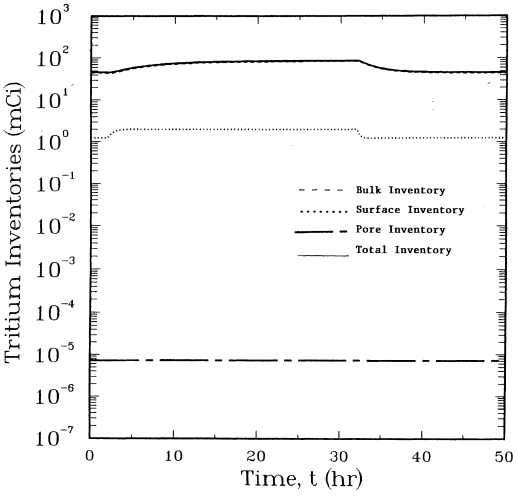

Fig. 8. The history of tritium inventory for a change in the sample temperature of 642–557–642°C.

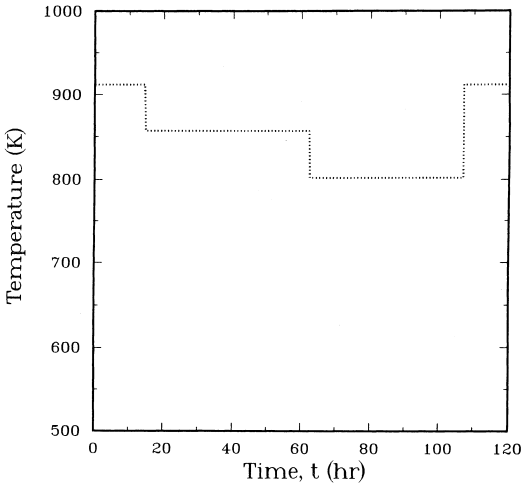

Fig. 9. Maximum temperature history for a sequence of temperature transients in the BEATRIX-II Phase II ring specimen.

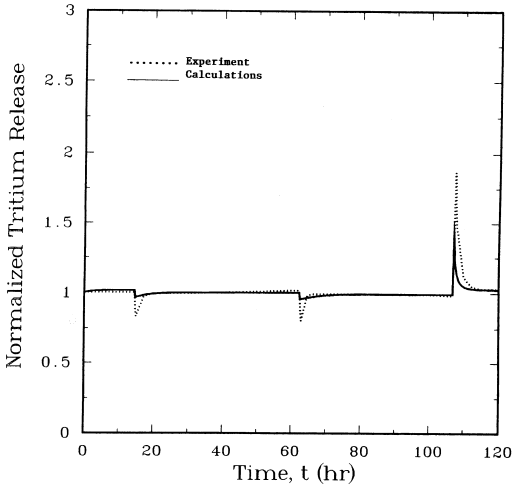

Fig. 11. Normalized tritium release history for the Phase II ring specimen during the temperature change sequence in a He + 0.01% H_2 purge gas.

temperature change sequence. Fig. 10 shows the calculated tritium release history for the temperature transients compared to the experimental release history. The calculated tritium release seems to be within the experimental uncertainties associated with the measured tritium release. The majority of the tritium inventory is found inside the bulk.

A second case analyzed had the same temperature transient as in Fig. 9. However, the purge gas contained 0.01% H_2 instead of 0.1% as in the previous case. Fig. 11 shows the calculated and measured tritium release histories for the temperature change sequence. The change in tritium release following each transient is less pronounced than in the previous case (Fig. 10). More than 90% of the calculated tritium inventory is found in the bulk. The inventory is about a factor of 2 more than that calculated for the previous case, which illustrates the importance of the addition of protium to the purge.

Due to the huge uncertainties in the experimental data in the cases of the purge gas composition transients, it is impossible to analyze the transient behavior of tritium in order to reproduce the experimental data under a change in purge gas composition.

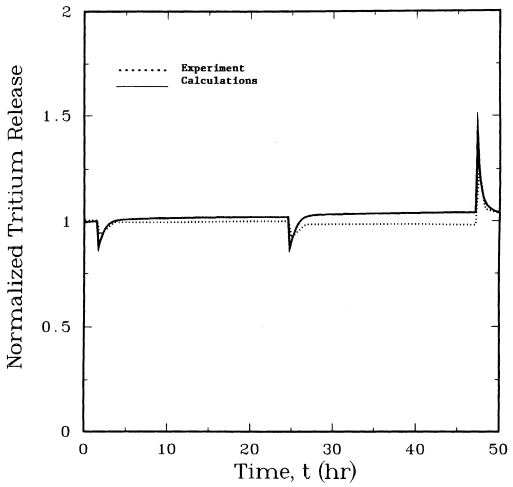

Fig. 10. Normalized tritium release history for the Phase II ring specimen during the temperature change sequence in a He + 0.1% H_2 purge gas.

4. Summary and conclusions

Due to the importance of understanding tritium behavior in the solid breeder material, a computer model (MISTRAL) was developed previously to predict the tritium release and inventory from a lithium-based ceramic solid breeder material. This model included the effect of several tritium transport mechanisms but neglected the effect of the dissolution flux fom the surface to the bulk and of trapping in the bulk. These could play an important role in some cases as suggested by the inability of the initial version of MISTRAL to reproduce the latest Li_2O experimental results from BEATRIX-II.

An important objective of this work was to account for the retention of the tritium in the bulk of the solid breeder. A model was developed in order to account for the kinetics of bulk trapping and detrapping of

tritium, and was included in the MISTRAL code to enable both steady and transient tritium analyses. A dissolution flux was then added to account for the tritium atoms going back to the bulk from the pore side and to provide a complete model for the surface processes. This capability was also implemented in the code, together with the capability of accounting for both first order and second order adsorption/desorption.

In order to check the validity of the code, it was used to analyze the Li_2O results from the BEATRIX-II experiment. The analysis was focused on the results from the ring specimens from Phases I and II of the experiment. It was divided into three phases:

1. Using the data available on the change of inventory due to different transients in order to obtain a set of input parameters that can reproduce the experimental values.
2. Verifying the obtained set of input parameters by comparing calculated end-of-life sample inventory to the experimental value.
3. Analysis of the transient tritium release history and comparison between the experimental values and the calculations.

From the above analysis and from parametric studies of the effects of the input parameters, the following indications emerged:

- Although Li_2O has a fast diffusion coefficient, most of the calculated tritium inventory was present in the bulk.
- The tritium inventory is strongly dependent on the activation energy of solution for reduced species.
- The tritium inventory for the cases analyzed showed no dependency on the heat of adsorption, the value of which is not known for Li_2O. This indicates that there is a possibility of predicting the inventory even without the accurate knowledge of some of the basic data.
- The new model added to MISTRAL was able to predict well within the experimental uncertainties the end of life inventory of the sample as well as the changes in inventory due to temperature transients. This indicates that tritium trapping represented here by formation and solubility of LiOT is the rate controlling process in Li_2O for the given set of conditions.
- Due to the huge effect of the adsorption in the stainless steel lines following purge gas composition transients, the code was not able to reproduce the experimental data for such transients. It can be seen from the analysis that most of the inventory change measured in the experiment is due to changes in the conditions in the lines and not in the sample. Although providing important information to modelers, such transients should be done very carefully to reduce the effect of the lines. For example, cases with pure helium which results in freeing activated surface sites in the lines should be avoided.
- For transient cases, the code results showed good agreement with the experimental data on the tritium release history in temperature transient cases.
- Reproduction of the BEATRIX-II ring specimen tritium release data required a detrapping rate constant about two orders of magnitude lower than the assumed initial value based on thermal decomposition of irradiated Li_2O. The latter value itself was lower than the value obtained from unirradiated LiOH decomposition experiments, suggesting that experimental conditions and irradiation level could play a role in determing this rate constant.
- The above results indicate the importance of including bulk trapping and detrapping in such a transient model in order to be able to better analyze cases such as the BEATRIX-II experiments. However, at this stage although the trapping model in the code is mathematically correct, the absence of data accurately characterizing the kinetics of LiOT formation and solubility and of the reverse process means that these results must be interpreted with caution. The model needs to be further refined in order to better include the kinetics of LiOT formation and solubility based on the local bulk conditions, as well as those of local LiOT precipitation based on bulk concentrations equivalent to the required moisture level. In parallel to this and to enable a better utilization of the features of such a model, an experimental effort is also required to provide data for a better characterization of the parameters defining the different rate equations.
- When considering all the uncertainties affecting transients, tritium release experiments in the short term should focus on well characterized quasi-steady state experiments where the end of life inventory following operation at well characterized conditions is measured.

Nomenclature

A_g	Surface area of the grain
$A_{s/g}$	Surface area associated with one grain
$C_g(r,t)$	Diffusive tritium concentration in the grain at position r and time t
$C_p^{(i)}(z,t)$	Concentration of species (i) in the pore at position z and time t
$C_{purge}^{(i)}$	Concentration of species (i) in the purge
$C_s(r,t)$	Concentration of tritium trapped in the grain at position r and time t
$D_g(T)$	Tritium diffusion coefficient in the grains
$D_{eff}^{(i)}$	Effective pore diffusion coefficient of species (i) in the pore
D_o	Pre-exponential for bulk diffusion
E_{ads}	Adsorption activation energy

E_β	Activation energy of adsorption from the bulk
E_{des}	Activation energy of desorption
E_{diff}	Activation energy of bulk diffusion
E_{diss}	Activation energy of dissolution
E_{s}	Activation energy of solution
f_{ads}	Multiple of adsorption flux
f_β	Multiple of bulk-to-surface flux
$\text{f}_{\text{D}_\text{p}}$	Multiple of pore diffusion coefficient
$G(t)$	Tritium generation rate at time t
$\text{G}_\text{p}^{(i)}(z,t)$	Volumetric source term of species (i) in the pore at position z and time t
h	Planck's constant
I_{old}	Mobile tritium inventory inside the grain at time t
I_{old}(trap)	Trapped tritium inventory at time t
k_{dsn}	LiOT decomposition rate constant from Eq. (28)
k_{tr}	Rate constant for tritium bulk trapping
k_{dtr}	Rate constant for tritium bulk detrapping
K_{equi}	Equilibrium constant for LiOT formation (Eq. (1))
K_{o}	Equilibrium constant for oxidized species reaction in the pore
K_{r}	Equilibrium constant for reduced species reaction in the pore
m	order of the surface processes
$M^{(i)}$	Molecular weight of species (i)
N_{avo}	Avogadro's number
N_{H}	Total number of protium atoms in the pore
N_{H_2}	Number of H_2 molecules in the pore
$N_{H_{2}\text{O}}$	Number of H_2O molecules in the pore
N_{HT}	Number of HT molecules in the pore
N_{HTO}	Number of HTO molecules in the pore
N_{O_2}	Number of O_2 molecules in the pore
N_{T}	Total number of tritium molecules in the pore
N_{T_2}	Number of T_2 molecules in the pore
$N_{\text{T}_2\text{O}}$	Number of T_2O molecules in the pore
N_{s}	Number of surface sites
Q	Heat of adsorption
r_{g}	Radius of the grain
R	Universal gas constant
T	Temperature
v_{g}	Grain volume
z_{adj}	Number of adjacent surface sites
$\mathscr{R}_{\text{ads}}$	Flux of atoms going to the surface from the pore
$\mathscr{R}_\beta$	Flux of tritium atoms going to the surface from the bulk
$\mathscr{R}_{\text{des}}$	Flux of atoms going to the pore from the surface
$\mathscr{R}_{\text{diss}}$	Flux of tritium atoms going to the bulk from the surface
ΔI	Change in inventory
θ	Total surface coverage
θ_T	Tritium surface coverage
σ	Condensation factor

References

[1] M.A. Abdou, E.L. Vold, C.Y. Gung, M.Z. Youssef, K. Shin, Fusion Technol. 9 (1986) 250.

[2] G. Federici, A.R. Raffray, M.A. Abdou, J. Nucl. Mater. 173 (1990) 185; G. Federici, PhD dissertation, University of California at Los Angeles, 1989.

[3] A.R. Raffray, S. Cho, M.A. Abdou, J. Nucl. Mater. 210 (1994) 143.

[4] M. Tetenbaum, A.K. Fischer, C.E. Johnson, Fusion Technol. 7 (1985) 53.

[5] O.D. Slagle, G.W. Hollenberg, BEATRIX-II Program 1990, Pacific Northwest Laboratory Report, PNL-7858 UC-423, 1991; O.D. Slagle, G.W. Hollenberg, T. Kurasawa, R.A. Verrall, BEATRIX-II: Phase I – First data transfer, Presented at Modelers and Code Development Meeting, Clearwater, FL, 1991.

[6] N.W. Gregory, R.H. Mohr, J. Am. Chem. Soc. 77 (1955) 2142.

[7] J. Berkowitz, D.J. Meschi, W.A. Chupka, J. Chem. Phys. 33 (1960) 553.

[8] A. Badawi, PhD dissertation, University of California, Los Angeles, 1993.

[9] M.A. Pick, K. Sonnenberg, J. Nucl. Mater. 131 (1985) 208.

[10] M. Boudart, H. Eyring et al., Physical Chemistry, Academic Press, New York, 1975, p. 362.

[11] A. Badawi, A.R. Raffray, A. Ying, M.A. Abdou, Fusion Technol. 19 (1991) 1532.

[12] M.C. Billone, H. Attaya, J.P. Kopasz, Modeling of tritium behavior in Li_2O, Argonne National Laboratory Report, ANL/FPP/TM-260, 1992.

[13] A. Badawi, A.R. Raffray, Analysis of surface fluxes of hydrogen species in lithium ceramics, UCLA Report, UCLA-FNT-50, 1991.

[14] M. Tetenbaum, C.E. Johnson, J. Nucl. Mater. 126 (1984) 25.

[15] J.F. Quanci, PhD dissertation, Princeton University, Princeton, NJ, 1989.

[16] G. Federici, A.R. Raffray, M.A. Abdou, J. Nucl. Mater. 173 (1990) 214.

[17] H. Katsuta, S. Kohishi, H. Yoshida, J. Nucl. Mater. 116 (1983) 244.

[18] S. O'hira, T. Hayashi, K. Okuno, H. Kudo, Fusion Eng. Design 8 (1989) 335.

[19] H. Kudo, K. Okuno, S. O'hira, J. Nucl. Mater. 155–157 (1988) 524.

[20] B.M.W. Trapnell et al., Chemisorption, 2nd ed., Butterworths, London, 1964.

[21] Minutes of the BEATRIX-II Modelers and Code Developers Meeting, JAERI Headquarters, Tokyo, 1992.

[22] A. Badawi, A.R. Raffray, M.A. Abdou, BEATRIX-II Phase 1 Li_2O tritium release data: results from initial analysis, presented in BEATRIX-II Modeler's and Code Developer's Meeting, Tokyo, 1992.

[23] M. Briec, in: G.W. Hollenberg, I.J. Hastings (Eds.), Advances in Ceramics, vol. 27, The American Ceramic Society, Westerville, OH, 1990, p. 360.

[24] H. Kwast, A. Kout, R.P. Muis, M.P. Stijkel, A.J. Flipot, J.D. Elen, Fusion Eng. Design 8 (1989) 359.
[25] R.A. Verrall, J.M. Miller, I.J. Hastings, D.S. MacDonald, D.H. Rose, in: G.W. Hollenberg, I.J. Hastings (Eds.), Advances in Ceramics, vol. 27, The American Ceramic Society, Westerville, OH, 1990, p. 41.
[26] H. Kudo, K. Tanaka, H. Amano, J. Inorg. Nucl. Chem. 40 (1978) 363.
[27] H. Kudo, J. Nucl. Mater. 87 (1979) 185.